Journal of Materials Processing Technology 209 (2009) 4502–4508

Contents lists available at ScienceDirect

Journal of Materials Processing Technology

journal homepage: www.elsevier.com/locate/jmatprotec

The influence of tool flank wear on residual stresses induced by milling aluminum alloy

Z.T. Tang[a,b,*], Z.Q. Liu[b], Y.Z. Pan[b], Y. Wan[b], X. Ai[b]

[a] School of Mechanical and Electrical Engineering & Automobile Engineering, Yantai University, PR China
[b] School of Mechanical Engineering, Shandong University, PR China

ARTICLE INFO

Article history:
Accepted 6 October 2008

Keywords:
Residual stresses
Flank wear
Cutting force
Cutting temperature
Aluminum alloy

ABSTRACT

The machining processes could induce residual stresses that enhance or impair greatly the performance of the machined component. Machining residual stresses correlate very closely with the cutting parameters and the tool geometries. In this paper, the effect of the tool flank wear on residual stresses profiles in milling of aluminum alloy 7050-T7451 was investigated. In the experiments, the residual stresses on the surface of the workpiece and in-depth were measured by using X-ray diffraction technique in combination with electro-polishing technique. In order to correlate the residual stresses with the thermal and mechanical phenomena developed during milling, the orthogonal components of the cutting forces were measured using a Kistler 9257A type three-component piezoelectric dynamometer. The temperature field of the machined workpiece surface was obtained with the combination of infrared thermal imaging system and finite element method. The results show that the tool flank wear has a significant effect on residual stresses profiles, especially superficial residual stress. As the tool flank wear length increases, the residual stress on the machined surface shifts obviously to tensile range, the residual compressive stress beneath the machined surface increases and the thickness of the residual stresses layer also increases. The magnitude and distributions of the residual stresses are closely correlated with cutting forces and temperature field. The three orthogonal components of the peak cutting forces increase and the highest temperature of the machined workpiece surface also increases significantly with an increase in the flank wear. The results reveal that the thermal load plays a significant role in the formation of the superficial residual stress, while the dominative factor that affects thickness of residual stresses layer is the mechanical load in high-speed milling aluminum alloy using worn tool.

1. Introduction

It is well known that machining processes create residual stresses on the surface of machined components. The machining residual stresses can have significant effects on component life by influencing fatigue strength, creep, and stress-corrosion-cracking resistance. In addition, machining-induced residual stresses can have detrimental effects on the component geometry and dimensional stability. Therefore, it is of considerable significance to optimize distributions of residual stresses by controlling the cutting conditions (Brinksmeier et al., 1982; Jacobus et al., 2000).

Machining residual stresses correlate very closely with the cutting parameters and the tool geometries. At present, numerous studies have been conducted by many researchers to determine relationships between the cutting conditions and residual stresses. Outeiro et al. (2002) studied the residual stress induced in turning of AISI 316L steel. Particular attention was paid to the influence of the cutting parameters, such as the cutting speed, feed and depth of cut. Patrik et al. (2004) investigated the influence of rake angle, cutting feed and cutting depth on residual stresses in hard turning AISI 52100, the results show that rake angle had the strongest influence on the residual stresses. The compressive stresses become greater with increased feed rate, while cutting depth had no obvious effect on residual stresses. Fuh and WU (1994) proposed the cutting speed, feed, tool nose radius and flank wear have the most significant effect on the residual stresses. Chen et al. (2004) developed a finite model to simulate the effects of tool flank wear and chip formation on residual stress when orthogonal cutting Ti–6Al–4V. Tonshoff et al. (2000) found that when turning hardened steels the residual stress magnitude on the surface shifts more toward the tensile region and into deeper depths with increasing flank wear length. Thiele et al. (2000) have found that tool-edge radius has a significant effect on surface residual stress and microstructure when finish hard turning

* Corresponding author at: School of Mechanical and Electrical Engineering & Automobile Engineering, Yantai University, PR China. Tel.: +86 531 88392045; fax: +86 531 88392045.
E-mail address: tangzhitao@gmail.com (Z.T. Tang).

0924-0136/$ – see front matter. Crown Copyright © 2008 Published by Elsevier B.V. All rights reserved.
doi:10.1016/j.jmatprotec.2008.10.034

Table 1
Chemical composition of 7050-7451 (% in weight).

Zn	6.7
Cu	2.5
Mg	2.3
Zr	0.12
Fe	0.13
Si	0.12
Mn	0.10
Ti	0.06
Others	0.15

AISI 52100 steel. The residual stresses in the axial and circumferential directions were more compressive with larger edge radius. Jang et al. (1996) studied the effects of different machining parameters (cutting speed, feed rate, depth of cut and tool-edge radius) on surface residual stress when turning AISI 304 stainless steel. Tool-edge radius was found to have the most significant effect on residual stress, where larger radius resulted in higher surface tensile residual stress in cutting direction. The authors reported that the effect of edge radius on inducing tensile residual stress in stainless steels is more noticeable than in other steels, and attributed this to the low thermal conductivity of stainless steels. In addition to the efforts above, other models have been proposed for correlating the residual stress with some cutting parameter (Jang et al., 1996; Lin et al., 1997, 2000; Jacobus et al., 2001; Capello, 2005; Liu et al., 2004; Mohamed et al., 2007; Outeiro et al., 2006; Jiang et al., 2006; Pawade et al., 2008). These research results revealed that the cutting tool geometry is the dominant factor determining the residual stresses profiles.

Although an extensive study on machining residual stress and their correlation with cutting parameters and tool geometries are available. But most researchers focus on the residual stresses in turning and grinding all kinds of steel materials. Not much attention is paid to the residual stresses in milling aluminum alloy. Moreover, the mechanism of formation of the machining residual stresses is not well correlated to important machining physical phenomena such as the dynamic cutting forces and cutting temperature field. The objective of this paper is to investigate experimentally the effect of tool wear on residual stresses in the milling of aluminum alloy 7050-T7451. To be able to correlate the residual stresses with the thermal and mechanical phenomena developed during milling, the cutting forces and the cutting temperature field were measured, respectively. At last, the formation of the residual stresses can be explained by the thermo-mechanical coupling effects.

2. Experiment

2.1. Experimental material

High-strength wrought aluminum alloy 7050-T7451 is widely used for aerospace application because of its combination of high strength, stress-corrosion-cracking resistance and toughness. The chemical composition and the mechanical properties of the material are presented in Table 1 and Table 2, respectively.

Table 2
Mechanical properties of 7050-T7451.

Yield strength (MPa)	455
Tensile strength (MPa)	510
Elongation (%)	10
Hardness (HB)	135
Young modulus (GPa)	71.7

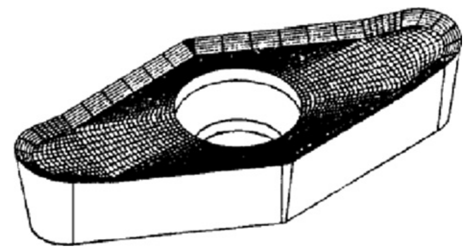

Fig. 1. Insert.

2.2. Experimental set-up

Milling tests were performed on a DECKEL MAHO DMU 70 V 5-axis universal machining center. Max power of the machine tool is 15 KW, and max spindle speed is 18,000 r/min. The workpiece was machined with superfine grain solid carbide inserts with 10,000 r/min spindle speed, 2 mm axial cutting depth, 10 mm radial cutting depth and 0.15 mm/z feed per tooth. The inserts VPGX2206EN-E10 (seen in Fig. 1) were mounted in corresponding arbor with a cutting diameter of 32 mm. The insert's rake and clearance angles are 25° and 6°, respectively. The tool flank wear was observed by a optics microscope (×100), seen in Fig. 2. In the experiment, the tool average flank wear length are 0.03, 0.07, 0.12, 0.17, 0.21, 0.26 mm, respectively. Dry cutting environment was used throughout the tests.

2.3. Residual stresses measurement

Residual stresses were measured by means of the X-ray diffraction method. Fig. 3 shows the used equipment, a portable stress analyzer from Stresstech Group's XSTRESS 3000. The main parameters of this apparatus are as follows: Cr tube (27 kV, 6 mA), 3 mm^2 measurement area, cross-correlation method for determining peak positions, Ni power calibration, 139.3° Bragg angle, ±6° ψ-oscillation, ±30° ϕ-oscillation. The location of the measurement point is at the center of the tool track. The stresses were measured parallel to the feed direction and perpendicular to the feed direction, respectively. In order to determine the in-depth residual stresses, the electro-polishing technique was used. The surface material was removed layer-by-layer using an electro-polishing machine Movipol-3 as shown in Fig. 4. The removed layer thickness can be determined using electronic digital micron indicator (seen in Fig. 5).

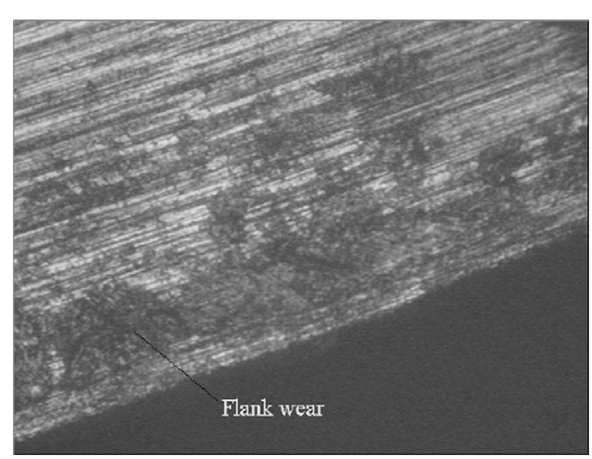

Fig. 2. Observation of flank wear.

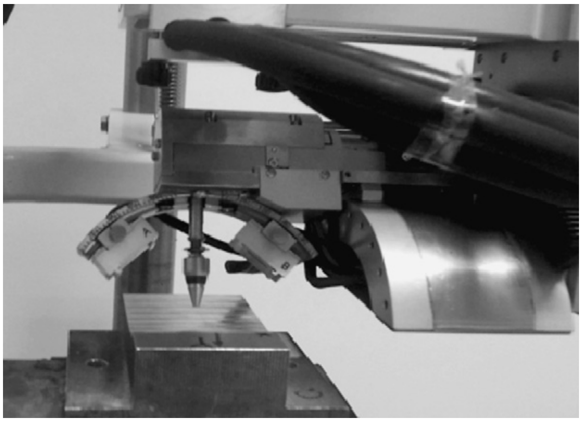

Fig. 3. X-ray stress Analyzer.

Fig. 4. Movipol-3electro-polishing machine.

2.4. Cutting force measurement

During milling process, a Kistler brand 9257 A-type three-component piezoelectric dynamometer under workpiece with the appropriate load amplifier was used for measuring three orthogonal cutting forces. The data acquisition software was used, which allows direct and continuous recording and simultaneous graphical visualization of the three orthogonal cutting forces. Diagram of measurement systems for cutting force are shown in Fig. 6.

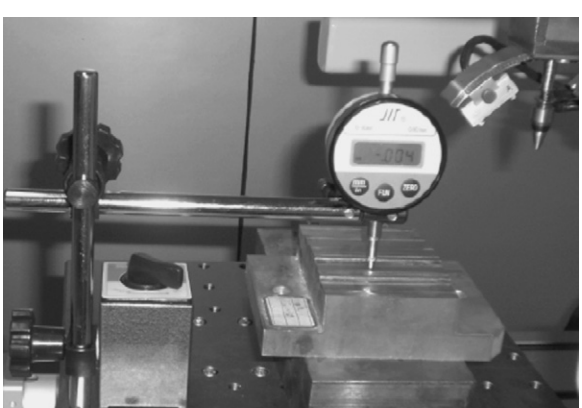

Fig. 5. Electronic digital micron indicator.

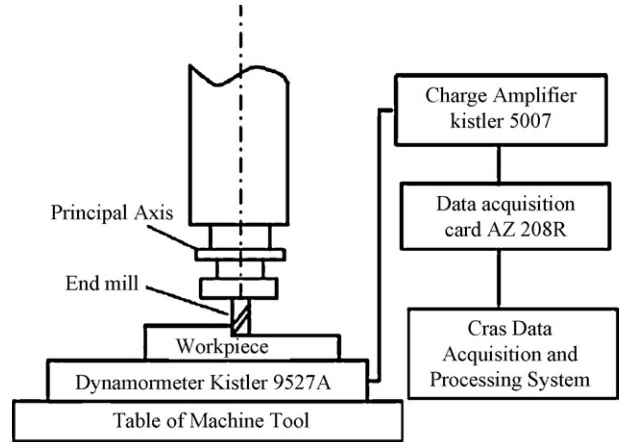

Fig. 6. Diagram of measurement systems for cutting forces.

2.5. Cutting temperature measurement

It is difficult to measure directly the cutting temperature by experiment. To obtain the temperature field of the machined workpiece surface, a method was presented with the combination of infrared thermal imaging system and finite element method. Fig. 7 shows that the flowchart of cutting temperature field prediction. Finite element method was used to predict cutting temperature field. The milling operation modeled was idealized by a single cutting tooth in a plane strain, orthogonal cutting because the axial cutting depth is five times more than feed per tooth. The FEA software DEFORM-2D^{TM}, a Lagrange implicit code, was used to simulate the machining of aluminum alloy 7050-T7451. As shown in Fig. 8, the finite element model with different flank wears was built. The workpiece was initially meshed with 18,000 isoparametric quadrilateral elements, while the tool, modeled as rigid, was meshed and subdivided into 5000 elements. For the sake of saving calculating time and memory space, the adapted meshing technology was used in simulation. The finer and smaller elements were considered in the contact area between tool and workpiece because a very large temperature gradient will occur in this region (Fang and Zeng, 2005). The model took into account dynamic effects, thermo-

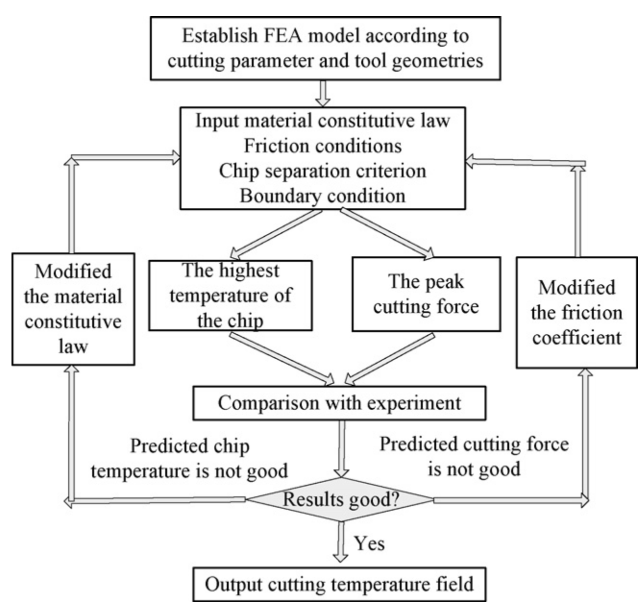

Fig. 7. Flowchart of cutting temperature field prediction.

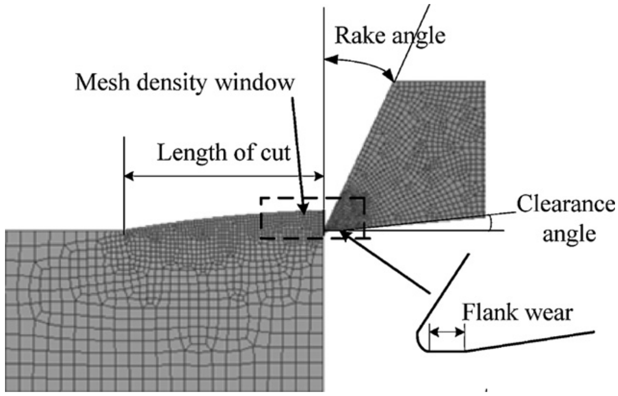

Fig. 8. Finite element model.

mechanical coupling, material constitutive equation, the damage law and contact with friction.

In order to validate the finite element model, the predicted and experimentally measured cutting forces and highest temperature of the chip were compared. The predicted values obtained by the finite element model can be adjusted by ever changing the simulation conditions such as the material constitutive law and friction conditions and so on. Fig. 9a and b show that the predicted *X* direction and *Y* direction peak cutting forces are 232.2 N and 117.8 N by FEM with flank wear of 0.03 mm, respectively. Fig. 10a and b show that the measured *X* direction and *Y* direction peak cutting forces are 248.9 N and 143.2 N by experiment, respectively. At the same time, the temperature of the chip during milling was measured by infrared thermal imaging system, seen in Fig. 11. The measured highest temperature of the chip is 245 °C, while the simulation value is 287.3 °C, seen in Fig. 12. The predicted peak cutting forces and highest chip temperature show a good agreement with the experiment results, which indicate that the simulation model is reasonable. Therefore, the model can be used to predict the temperature of the machined workpiece surface.

Fig. 12 shows the temperature field of the machined workpiece surface with flank wear of 0.03 mm. The cutting temperature fields in other flank wears can be also obtained by this model.

3. Results

X-ray diffraction measurements were taken at four different points on the surface. Effects of the tool flank wear on superficial residual stresses were presented in Fig. 13. S11 and S22 designate the measured residual stress parallel to and normal to the feed direction, respectively. From this figure, it is noted that the superficial residual stresses are most strongly correlated to the tool flank wear. It can be seen that the small flank wear produced a lower tensile or compressive stresses near the surface, and the stresses transformed to the tensile residual stress states with an increase in

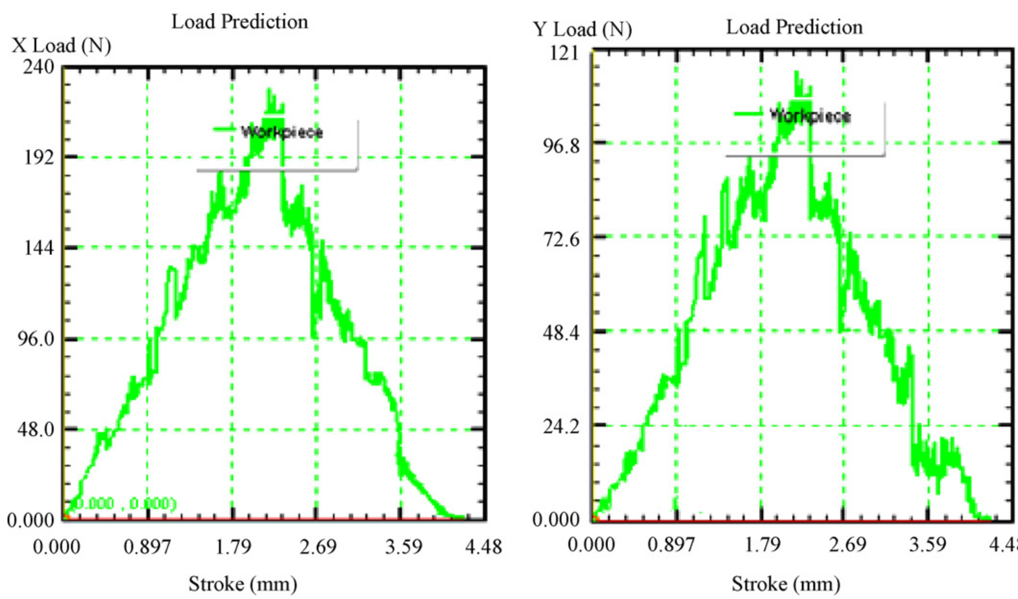

(a) X direction cutting force (b) Y direction cutting force

Fig. 9. The predicted cutting force by FEM.

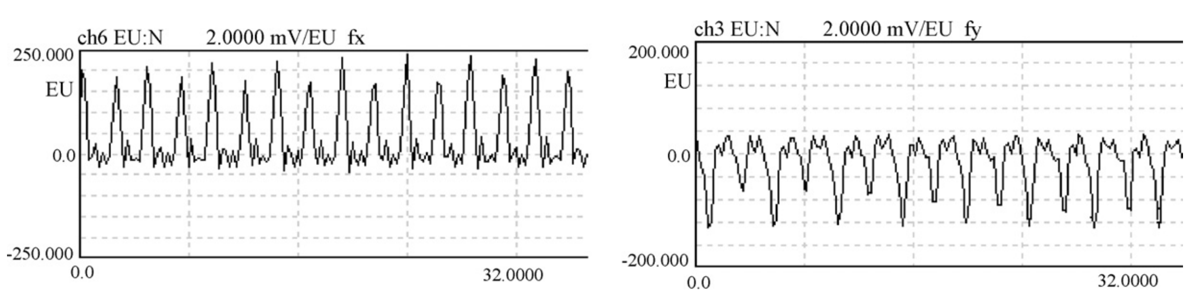

(a) X direction cutting force (b) Y direction cutting force

Fig. 10. The measured cutting force by experiment.

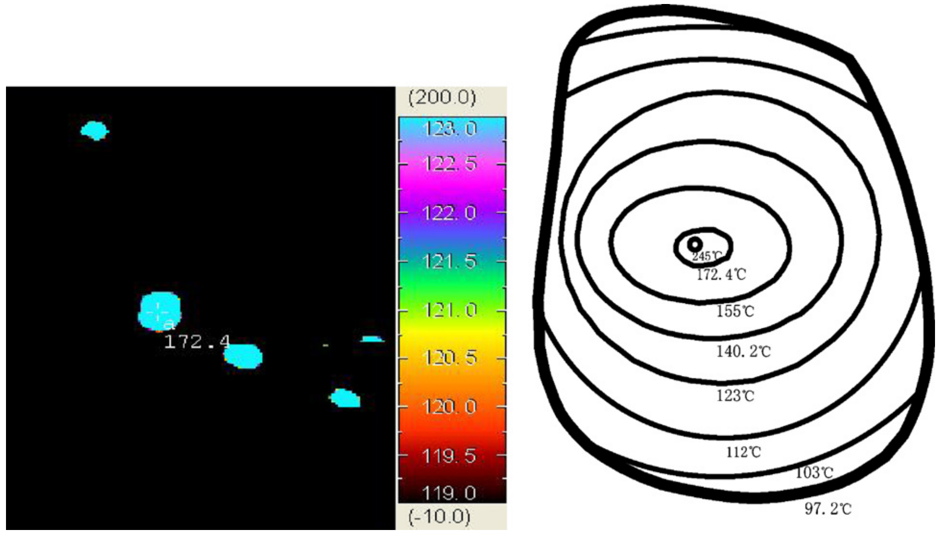

Fig. 11. The chip temperature measured by experiment.

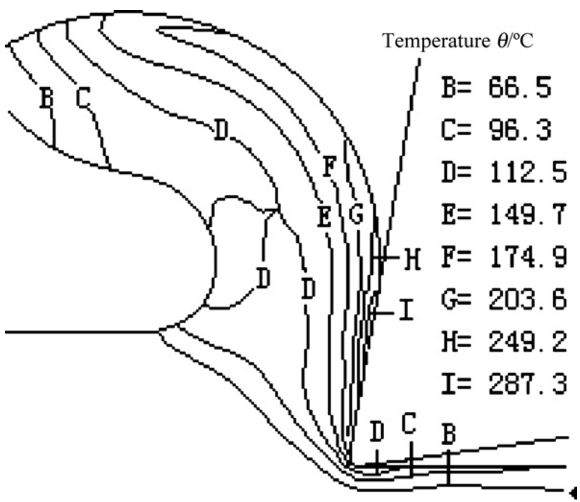

Fig. 12. The temperature field obtained by FEM.

the flank wear. It can be also seen that the residual stresses change in different measurement location. Different flank wear lead to different residual stress scatter and the large flank wear also produced more scatter in the data.

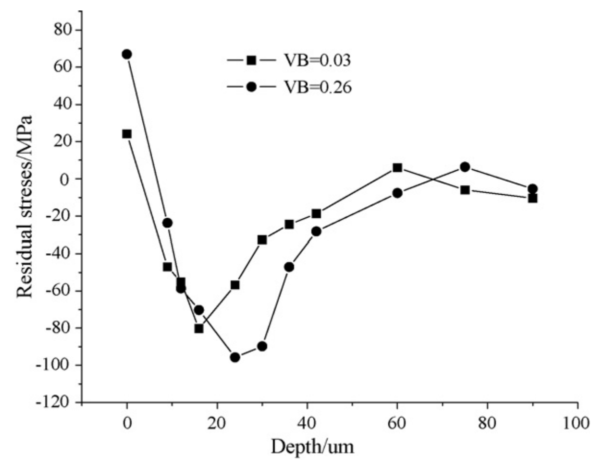

Fig. 14. Effects of flank wear on in-depth residual stresses parallel to feed direction.

The measurement results for reisual stresses depth profiles were presented in Figs. 14 and 15. From these figures, it is noted that the similar residual stresses varience tendency can be observed, that is, the residual stresses are tensile on the surface and fall off to a maximum compressive states with an increase in-depth, after

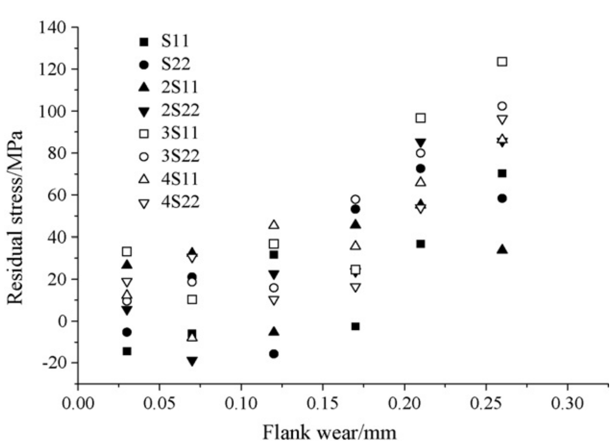

Fig. 13. Effects of flank wear on superficial residual stresses for four different measurement points.

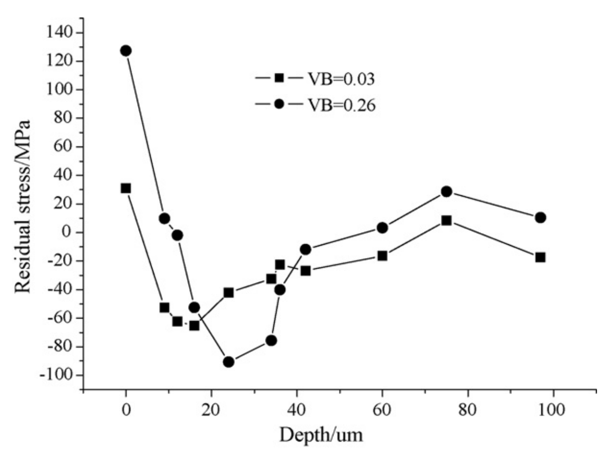

Fig. 15. Effects of flank wear on in-depth residual stresses perpendicular to feed direction.

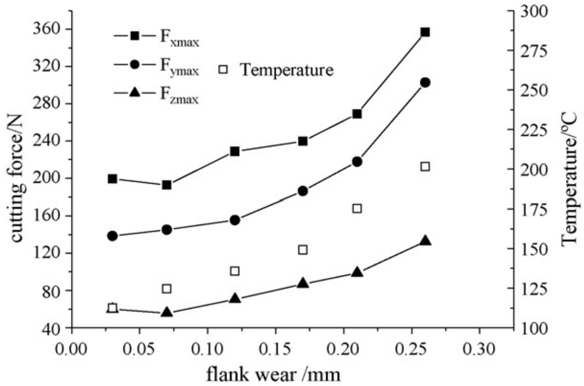

Fig. 16. Effects of flank wear on peak cutting forces and the highest temperature of the machined workpiece.

which compressive residual stresses transform to tensile states, and the residual stresses approach a steady value in near workpiece substrate. The maximun compressive stresses occurred at the depth of 15–25 μm depending on the measured direciton and flank wear.Fig. 14 shows that the influence of flank wear on the residual stress depth profiles parallel to feed direction. It is noted that superficial residual stress increases from 24.1 to 66.9 MPa when the tool flank wear increases from 0.03 to 0.26 mm. The residual compressive stress beneath the machined surface increases and the thickness of the residual stresses layer also increases. Fig. 15 shows that the influence of flank wear on the residual stress depth profiles perpendicular to feed direction. The flank wear has a significant effect on superficial residual stress. The superficial residual stress sharp increases from 31.2 to 127.3 MPa when the tool flank wear increases from 0.03 to 0.26 mm. Similarly, the maximum compressive residual stress and the thickness of the residual stresses layer also increases with an increase in the flank wear.

In order to explain the residual stress tendency, when milling aluminum alloy for different flank wears, three orthogonal components of the measured cutting forces are shown in Fig. 16. The highest cutting temperature of the surface of machined workpiece is also shown in Fig. 16. As seen, three orthogonal components of peak cutting forces and the highest cutting temperature all increase with an increase in the flank wear. When the flank wear length is above 0.21 mm, cutting forces and temperature change significantly. These subsequently influence the magnitude and distributions of the residual stresses.

4. Discussion

It is known that the thermally dominant machining deformation leaves behind tensile residual stresses in the machined surface, whereas mechanically dominant machining deformation induces compressive residual stress (Sharman et al., 2006). In this study, when the tool flank wear increases, the highest temperature of the machined workpiece surface increases significantly, resulting in the rise of the tensile residual stress on the surface of the workpiece. At the same time, the increases of three orthogonal components of peak cutting forces induce compressive residual stress. Therefore, it means the thermal load plays a significant role in the formation of the superficial residual stresses in high-speed milling aluminum alloy using worn tool. However, the dominative factor that affects thickness of residual stresses layer is the cutting force, because the regions affected by the thermal load are shallow compared with that affected by the mechanical load. This reveals that a decrease of the thickness of residual stresses layer with a higher cutting speed are mainly due to a decrease in the cutting forces that result in a smaller plastic deformation zone.

5. Conclusions

This paper study the effect of tool wear on residual stresses profiles in the milling of aluminum alloy 7050-T7451. To be able to correlate the residual stresses with the thermal and mechanical phenomena developed during milling, the cutting forces and the cutting temperature field were measured, respectively. The following conclusions can be drawn:

(1) The tool flank wear have a significant effect on superficial residual stresses, the small flank wear produced a lower tensile or compressive stresses on the surface, and the stresses shift obviously to tensile state with an increase in the flank wear. The large flank wear produced more scatter in the stress data.
(2) The similar residual stress depth profiles can be observed, that is, the superficial residual stresses are the lower tensile or compressive and fall off to a maximum compressive states with an increase in-depth, after which compressive residual stresses approach a steady value in near workpiece substrate. When the tool flank wear increases, the residual compressive stress beneath the machined surface increases and the thickness of the residual stresses layer also increases.
(3) Three orthogonal components of peak cutting forces and the highest cutting temperature all increase with an increase in the flank wear. When the flank wear length is above 0.21 mm, cutting forces and temperature change significantly with an increase in the flank wear.
(4) The thermal load plays a significant role in the formation of the superficial residual stresses in high-speed milling aluminum alloy using worn tool. However, the dominative factor that affects thickness of residual stresses layer is the mechanical load.

Acknowledgements

This topic of research is supported by the Natural Science Foundation of China under Grant Nos. 50435020, 50675122 and 50828501.

References

Brinksmeier, E., Gammett, J.T., Koenig, W., 1982. Residual stresses—measurement and causes in machining process. Ann. CIRP 31, 491–510.

Capello, E., 2005. Residual stress in turning Part I: influence of process parameters. J. Mater. Process. Technol. 160, 221–228.

Chen, L., El-Wardany, T.I., Harris, W.C., 2004. Modeling the effects of flank wear land and chip formation on residual stress. Ann. CIRP 53, 95–98.

Fang, G., Zeng, P., 2005. Three-dimensional thermo-elastic-plastic coupled FEM simulations for metal oblique cutting processes. J. Mater. Process. Technol. 168, 42–48.

Fuh, K.H., W.U., C.F., 1994. A residual-stress model for the milling of aluminum alloy (2014-T6). J. Mater. Process. Technol. 51, 87–105.

Jacobus, K., Devor, R.E., Kapoor, S.G., 2000. Machining induced residual stress: experimentation and modeling. Trans. ASME, J. Manuf. Sci. Eng. 122, 20–31.

Jacobus, K., Kapoor, S.G., Devor, R.E., 2001. Experimentation on the residual stresses generate by endmilling. Trans. ASME, J. Manuf. Sci. Eng. 123, 748–752.

Jiang, H., Domenico, U., Rajiv, S., 2006. Investigation of cutting conditions and cutting edge preparations for enhanced compressive subsurface residual stress in the hard turning of bearing steel. J. Mater. Process. Technol. 171, 180–187.

Jang, D.Y., Watkins, T.R., Kozaczek, K.J., 1996. Surface residual stresses in machined austenitic stainless steel. Wear 194, 168–173.

Lin, Z.C., Lai, W.L., Lin, H.Y., Liu, C.R., 1997. Residual stresses with different tool flank wear lengths in the ultra-precision machining of Ni–P alloys. J. Mater. Process. Technol. 65, 116–126.

Lin, Z.C., Lai, W.L., Lin, H.Y., Liu, C.R., 2000. The study of ultra-precision machining and residual stress for NiP alloy with different cutting speeds and depth of cut. J. Mater. Process. Technol. 97, 200–210.

Liu, M., Talagi, J.I., Tsukuda, A., 2004. Effect of tool nose radius and tool wear on residual stress distribution in hard turning of bearing steel. J. Mater. Process. Technol. 150, 234–241.

Mohamed, N.A.N., Ng, E.G., Elbestawi, M.A., 2007. Modeling the effects of tool-edge radius on residual stresses when orthogonal cutting AISI 316L. Int. J. Mach. Tools Manuf. 47, 401–411.

Outeiro, J.C., Dias, A.M., Lebrun, J.L., Astakhov, V.P., 2002. Machining residual stresses in AISI 316L steel and their correlation with the cutting parameters. Mach. Sci. Technol. 6, 251–270.

Outeiro, J.C., Umbrello, D., M'Saoubi, R.M., 2006. Experimental and numerical modeling of the residual stresses induced in orthogonal cutting of AISI 316L steel. Int. J. Mach. Tools Manuf. 46, 1786–1794.

Patrik, D., Fredrik, G., Michael, J., 2004. The influence of rake angle, cutting feed and cutting depth on residual stresses in hard turning. J. Mater. Process. Technol. 147, 181–218.

Pawade, R.S., Joshi, S.S., Brahmankar, P.K., 2008. Effect of machining parameters and cutting edge geometry on surface integrity of high-speed turned Inconel 718. Int. J. Mach. Tools Manuf. 48, 15–28.

Sharman, A.R.C., Hughes, J.I., Ridgway, K., 2006. An analysis of the residual stresses generated in Inconel 718^{TM} when turning. J. Mater. Process. Technol. 173, 359–367.

Thiele, J.D., Melkote, S.N., Peascoe, R.A., 2000. Effect of cutting-edge geometry and workpiece hardness on surface residual stresses in finish hard turning of AISI 51200 steel. Trans. ASME, J. Manuf. Sci. Eng. 122, 642–649.

Tonshoff, H.K., Arendt, C., Amor, R.B., 2000. Cutting of hardened steel. Ann. CIRP 49, 547–566.